The mouse HP1 proteins are not required for cell viability but are essential for preventing liver tumorigenesis

Nehmé Saksouk[1-4*], Shefqet Hajdari[1-4*], Marine Pratlong[5], Célia Barrachina[5], Aliki Zavoriti[1-4], Amélie Sarrazin[6], Nelly Pirot[1-4], Jean-Yohan Noël[1-4], Lakhdar Khellaf[4], Eric Fabbrizio[1-4, 7], Florence M. Cammas[1-4, 7]

[1] IRCM, Institut de Recherche en Cancérologie de Montpellier, Montpellier, F-34298, France.

[2] INSERM, U1194, Montpellier, F-34298, France.

[3] Université de Montpellier, Montpellier, F-34090, France.

[4] Institut régional du Cancer de Montpellier, Montpellier, F-34298, France.

[5] MGX, Biocampus Montpellier, CNRS, INSERM, Univ Montpellier, Montpellier, France

[6] MRI, BioCampus Montpellier, CNRS, INSERM, Univ Montpellier, Montpellier, France

[7] CNRS, Route de Mende, Montpellier, France

Corresponding author: Florence Cammas, Florence.cammas@inserm.fr

* Contributed equally to the work

Abstract

Chromatin organization plays essential roles in cell identity and functions. Here, we demonstrated by hepatocyte-specific inactivation of the genes encoding the three Heterochromatin Protein 1 (HP1α, β and γ) in mice (HP1-TKO) that these proteins are dispensable for hepatocyte activity and survival. Conversely, the chronic absence of these proteins led to a drastic increased incidence of liver tumor development. Molecular characterization of HP1-TKO hepatocytes revealed that HP1 proteins are required for maintenance of histone marks associated with heterochromatin, and for the appropriate expression of large number of genes involved in liver-specific functions as well as in genes encoding for transcriptional repressors of the KRAB-ZFP family. Moreover, several specific endogenous retrovirus families were upregulated in HP1-TKO hepatocytes, leading to the deregulated expression of genes in their vicinity. Our findings indicate that HP1 proteins act as guardians of liver homeostasis to prevent tumor development through the modulation of multiple chromatin-associated events.

Keywords: chromatin; HP1; cancer; liver; transcriptional silencing; endogenous retrovirus

Introduction

Chromatin is a large structure that is made of DNA fibers associated with histone proteins, and that is essential for the interpretation of genetic information in a cell-type and tissue-specific manner (Jenuwein and Allis 2001). Its alterations can have devastating consequences, as evidenced by the large number of diseases induced by mutations in chromatin-associated proteins (Koschmann et al. 2017; Mirabella et al. 2016), as well as by the dramatic changes in chromatin organization observed in cancer cells (Stein et al. 2000). Although extensively studied in the past three decades, it is still largely unknown how chromatin organization is regulated and involved in whole organism homeostasis.

Chromatin can be divided, according to its structural and functional features, in euchromatin and heterochromatin. Euchromatin displays low compaction level, is highly enriched in genes, and is transcriptionally competent. Conversely heterochromatin is highly compacted, enriched in repetitive DNA sequences, and mostly silent. Although, heterochromatin was considered for a long time as an inert compartment with the single function of silencing parasite DNA sequences, it is now recognized as a dynamic and functional compartment (Janssen et al. 2018a). Heterochromatin Protein 1 (HP1) proteins were first isolated as major heterochromatin components in *Drosophila* (James and Elgin 1986), and they are highly conserved from yeast to mammals which express three isoforms (HP1α, HP1β and HP1γ). These proteins are characterized by an N-terminal chromodomain (CD), which is involved in the recognition of the heterochromatin-associated histone mark H3 lysine-9 di- or trimethylated (H3K9me2/3), and a C-terminal chromoshadow domain (CSD), which constitutes a platform for interaction with many protein partners. These two domains are separated by the hinge domain that is crucial for HP1 association with RNA and recruitment to heterochromatin (Eissenberg and Elgin 2014; Lomberk et al. 2006). Thus, HP1 proteins are at the crossroads of the structural and functional organization of chromatin. Accordingly, HP1 are important for heterochromatin silencing, chromosome segregation, regulation of gene expression, DNA repair and DNA replication (Dinant and Luijsterburg

2009; Fanti and Pimpinelli 2008; Nishibuchi and Nakayama 2014). Moreover, HP1 proteins are essential for embryonic development in several organisms, including *Drosophila* (Eissenberg et al. 1992), C. *elegans* (Schott et al. 2006) and the mouse (our unpublished data). HP1α is essential for the plasticity of T helper (Th2) lymphocytes (Allan et al. 2012), HP1β for neuro-muscular junctions (Aucott et al. 2008) and HP1γ for spermatogenesis (Abe et al. 2011; Brown et al. 2010). Several studies also suggested a correlation between HP1 expression level and cancer development and/or metastasis formation; however, HP1 role in tumorigenesis remains to be clarified (Dialynas et al. 2008; Vad-Nielsen and Nielsen 2015).

To assess the functions of this family of proteins in homeostasis and to bypass the embryonic lethality of their genetic ablation, we inactivated all HP1 encoding genes in mouse hepatocytes (HP1-TKO mice). Liver chromatin organization has been well characterized in several physio-pathological conditions (Janssen et al. 2018b). In addition, several known HP1 partners, including the transcription cofactors TRIM24 and TRIM28, and the histone-lysine N-methyltransferase SUV39H1, play key roles in hepatocytes. Therefore, hepatocytes constitute an excellent model to investigate HP1 roles in chromatin functions ((Herquel et al. 2011; Fan et al. 2013; Bojkowska et al. 2012a; Khetchoumian et al. 2007; Hardy and Mann 2016)). Unexpectedly, we found that in HP1-TKO mice, hepatocytes can differentiate and contribute to liver functions throughout life. Conversely, HP1 proteins are critical for preventing liver tumorigenesis. Finally, molecular characterization of HP1-TKO mice revealed that HP1 are involved in the regulation of heterochromatin organization and of the expression of genes and Endogenous Retroviruses (ERV). Altogether, these data highlight a new function of HP1 proteins as guardians of liver homeostasis through the modulation of various chromatin-associated events.

RESULTS

HP1 proteins are not required for hepatocyte proliferation and survival

To unravel HP1 functions in homeostasis, the HP1β and HP1γ encoding-genes (*Cbx1* and *Cbx3,* respectively) were inactivated in the liver of HP1αKO mice (Allan et al. 2012) using the Cre recombinase expressed under the control of the hepatocyte-specific albumin promoter (Postic et al. 1999) (Fig. 1A). These animals were called HP1-TKO. Liver-specific excision of the *Cbx1* and *Cbx3* alleles was confirmed by PCR (Fig. 1B), and the absence of HP1β and HP1γ protein expression was checked by western blotting. At 7 weeks post-partum as well as at middle-aged, the overall level of HP1β and HP1γ was decreased by about 60% in HP1-TKO liver (Fig. 1C). Furthermore, immuno-fluorescence analysis of liver cryosections using anti-HP1β and -HP1γ antibodies showed that their expression was lost in about 60% of liver cells in HP1-TKO mice compared with controls (wild type littermates or age-matched wild type animals) (Fig. 1D). As this percentage corresponds to the hepatocyte fraction within the liver, these findings indicate that both proteins were concomitantly depleted in most hepatocytes. As expected since *Cbx5* (the HP1α-encoding gene) was knocked out in all body cells HP1α could not be detected HP1-TKO liver (Fig. 1B-C). Histological analysis of paraffin-embedded liver tissue sections of 7-week-old (young) and 3-6-month-old (middle-aged) control and HP1-TKO animals after hematoxylin/eosin/Safran staining did not reveal any significant difference in the structural organization/morphology of hepatocytes and of the parenchyma (Supplementary Figure 1). In agreement, analysis by immunohistochemistry (IHC) of Tissue Micro Arrays (TMA) made of liver samples using anti-Ki67 and anti-activated caspase 3 antibodies did not reveal any significant difference in cell proliferation and apoptosis in young and middle-aged HP1-TKO and control mice (Fig. 1E-F). As HP1 have been shown to play critical roles in genome stability (Shi et al. 2008; Bosch-Presegué et al. 2017), IHC was performed also with an antibody against the phosphorylated form of H2AX (γH2AX), a marker of DNA damage (Kuo and Yang 2008). However, the number of γH2AX-

positive cells was not significantly different in livers from young and middle-aged HP1-TKO and control animals (Fig. 1G), suggesting that HP1 proteins are not crucial for the DNA damage response in liver. These data demonstrated that in the mouse, the three HP1 proteins are dispensable for the appropriate structural organization and function of hepatocytes throughout life.

Heterochromatin organization is altered in HP1-TKO hepatocytes

To determine the effect of the absence of HP1 on heterochromatin organization in hepatocytes, first the level of different heterochromatin-associated histone marks was investigated by western blotting. H3K9me3 and H4K20me3, two marks of constitutive heterochromatin, were strongly decreased in the liver of 7-week-old and 3-6-month-old (middle-aged) HP1-TKO mice compared with age-matched controls. Conversely, no change of H3K27me3, a facultative heterochromatin mark, and of H3K9me2, H4K20me2 and H4K20me1 was observed (Fig. 2A). Although these results suggested that the absence of the three HP1 proteins affected heterochromatin organization, chromocenters (i.e., DAPI-dense structures that contain structural components of heterochromatin) still clustered, but tended to be more associated with the nuclear periphery in HP1-TKO hepatocytes (Fig. 2B). To precisely quantify the distribution of chromocenters, nuclei were divided in four co-centric areas in which the intensity of DAPI staining was measured using the cell profiler software (schema in Fig. 2C). In control nuclei, DAPI staining was roughly homogeneously distributed in the four areas (Fig. 2B-C). Conversely, in HP1-TKO nuclei, it increased progressively from the inner part to the external part. This indicated that in the absence of HP1α, β and γ, heterochromatin tended to be more associated with the nuclear periphery. In mammals, HP1-associated heterochromatin is mainly around centromeres, in pericentromeric heterochromatin. This region is mostly made of about 200 000 tandem repeats of a 234bp sequence (called major satellite in mice (Martens et al. 2005) and gives rise to a low level of transcripts that remain associated with chromatin for its maintenance (Velazquez Camacho

et al. 2017). In HP1-TKO livers, major satellite repeat expression was slightly, but not significantly decreased compared with control livers (Fig. 2D). Consistent with the loss of H3K9me3, chromatin immunoprecipitation (ChIP) experiments showed that this mark was decreased at the major satellite sequences in HP1-TKO compared with control livers (Fig. 2E). These data indicated that in hepatocytes, HP1 proteins are essential for the structural organization of constitutive heterochromatin, but not for the regulation of major satellite expression.

HP1 proteins are involved in the regulation of liver-specific gene expression programs

Previous reports suggested that HP1 proteins are also involved in the regulation of gene expression (Eissenberg and Elgin 2014). To investigate the effect of HP1 loss on gene expression, an unbiased RNA-seq transcriptomic analysis was performed on libraries prepared from 7 week-old control and HP1-TKO liver RNA. This analysis showed that 1215 genes were differentially expressed between control and HP1-TKO liver samples (with a 1.5-fold threshold difference and an adjusted $P \leq 0.05$) (Fig. 3A). As expected on the basis of the established HP1 role as gene silencers in several cellular and animal models and the loss of the repressive H3K9me3 mark (this study), more genes were upregulated (730; 5.1% of all genes detected in the RNA-seq analysis, Supplementary Table 1) than downregulated (485; 3.4% of all genes detected in the RNA-seq analysis, Supplementary Table 1) in HP1-TKO compared with control livers. These genes were distributed throughout the genome without preferential chromosomal location, compared with the global gene distribution (Supplementary Figure 2).

Analysis of the differentially expressed genes (HP1-dependent genes) using the David Gene Ontology (https://david.ncifcrf.gov/) and Gene Set Enrichment Analysis (GSEA; http://software.broadinstitute.org/gsea/index.jsp) programs revealed that several biological

processes were significantly affected in HP1-TKO liver, including the endoplasmic reticulum (ER) and reduction-oxidation (redox) processes (Fig. 3B & Supplementary Tables 2 & 3). In agreement with data showing a link between the levels of reactive oxygen species (ROS) and redox (Zeeshan et al. 2016), genes encoding cytochrome P450 (CYP) family members, which play crucial roles in these processes, were significantly enriched among the HP1-dependent genes (for instance, 11 members of the CYP2 family involved in ER and redox functions) (Bhattacharyya et al. 2014; Park et al. 2014). Moreover, *Nox4*, the gene encoding the nicotinamide adenine dinucleotide phosphate (NADPH) oxidase isoform most consistently associated with ER and ROS in liver (Paik et al. 2014), was significantly downregulated in HP1-TKO compared with control livers (Fig. 3C & Supplementary Table 1). In agreement with the link between ROS production and liver inflammation (Cichoż-Lach and Michalak 2014), *Ifit2*, the gene encoding interferon-induced protein with tetratricopeptide repeats 2 was upregulated in HP1-TKO livers (Fig. 3B-C & Supplementary Table 4). The RNA-seq data analysis also showed a significant enrichment in genes involved in other liver specific functions, such as steroid hormone biosynthesis, and drug and lipid metabolic processes (Fig. 3B and Supplementary Table 5). In agreement, among the 193 genes with liver-specific expression according to the Tissue Specific Gene Expression and Regulation software (bioinfo.wilmer.jhu.edu/tiger), 6.7% were upregulated and 8.3% downregulated in HP1-TKO livers compared with 5.1% and 3.4% for the full set of genes. This suggested that HP1 proteins have important functions in the modulation of genes involved in liver homeostasis (Supplementary Table 6). The differential expression of *Cyp2c29* and *Cyp2b10* (ER and redox), *Ifit2* (interferon γ signature) and *Nox4* (ROS production) was validated by RT-qPCR in 7 week-old HP1-TKO and age-matched control livers (Fig. 3C). These data demonstrated that although the liver of HP1-TKO animals did not display any significant phenotypical abnormality, HP1 proteins are required for regulating directly or indirectly the expression of several genes with key functions in liver homeostasis.

HP1 proteins are essential for silencing specific endogenous retroviruses

Genes encoding Krüppel Associated Box (KRAB) domain-containing proteins were the most enriched among the genes that were differentially expressed between HP1-TKO and control mice (*P* = 5.8E-26) (Fig. 3B & Supplementary Tables 1 & 2). The KRAB domain is almost exclusively present in the KRAB-Zinc Finger Protein (KRAB-ZFP) family of transcriptional repressors that are still actively evolving in mammals (Yang et al. 2017). The upregulation of several of these genes (*Rsl1*, *Zfp345*, *Zfp445* and *Zkscan3*) in 7-week-old HP1-TKO livers compared with age-matched controls was validated by RT-qPCR (Fig. 3C).

Beside themselves through an auto-regulatory loop, KRAB-ZFP members target also endogenous retroviruses (ERV) (Yang et al. 2017; O'Geen et al. 2007). Therefore, the expression of DNA repeats was investigated in our RNA-seq dataset. The coordinates of all annotated DNA repeats of the RepeatMasker database (mm10 assembly) were aligned against the RNA-seq reads and only those that could be assigned unambiguously to a specific genomic locus were analyzed. In total, 846 repeats were deregulated in HP1-TKO livers compared with control livers: 603 (71.3%) were upregulated and 243 (28.7%) downregulated (Fig. 4A & Supplementary Table 7). Moreover, among the upregulated repeats, 59.4% were Long Terminal Repeat (LTR) retrotransposons, ERV and 28.5% non-LTR retrotransposons (i.e., 19.2% long interspersed nuclear elements, LINEs, and 9.3% short interspersed elements, SINEs). The genome-wide distribution of these elements was 26.8% ERVs, 45.1% LINEs and 17.3% SINEs (Fig. 4B & Supplementary Table 7). This strongly supports the hypothesis that HP1 proteins are preferentially involved in ERV silencing.

To determine whether the differential expression of such repeats in HP1-TKO livers was associated with deregulation of gene expression, a map of HP1-dependent repeats located in the vicinity of HP1-dependent genes was first generated. To this end, 100kb were added on both sides of each HP1-dependent gene, and the HP1-dependent repeats present in

these regions were scored. This analysis showed that a fraction of HP1-dependent genes (138 upregulated and 94 downregulated) was associated with HP1-dependent repeats. Amongst the 138 upregulated genes, 116 were associated with 328 upregulated repeats, and 22 with 43 downregulated repeats. Among the 94 downregulated genes, 23 were associated with 40 upregulated repeats, and 71 with 157 downregulated repeats (Fig. 4C & Supplementary Tables 8 & 9). This analysis strongly suggested a link between HP1-dependent repeat expression and HP1-dependent gene expression. Moreover, HP1-dependent ERVs associated with upregulated genes belonged mainly to the ERV1 and ERVK sub-families, whereas ERVL and ERVL-MaLR members were underrepresented relative to their genome-wide distribution (Fig. 4D). Analysis of the distance between HP1-dependent genes and HP1-dependent repeats showed that upregulated repeats tended to be located closer to upregulated genes rather than to downregulated genes, whereas downregulated repeats tended to be located closer to downregulated genes. As a control, the alignment of all annotated repeats against HP1-dependent genes showed that repeats were homogeneously distributed in the regions surrounding both upregulated and downregulated genes (Fig. 4E). Amongst the deregulated genes associated with deregulated repeats, several have already been shown to be controlled by ERVs (i.e., *Mbd1*, *Bglap3*, *Obpa*, *Bmyc*, *Fbxw19* and *Zfp445*) (Ecco et al. 2016; Herquel et al. 2013). Interestingly, *Zfp445* was associated with four upregulated MERK26-int repeats that were at nearly equal distance between this gene and *Zkscan7,* another KRAB-ZFP-encoding gene also upregulated in HP1-TKO liver. This suggested that the reactivation of these specific repeats might interfere with the expression of both genes (Fig. 4F).

Altogether, these data highlighted the association between the deregulation of some HP1-dependent ERVs and of HP1-dependent genes in their vicinity. These results could seem paradoxical with the increased expression of several KRAB-ZFPs that are known to be involved in ERV silencing; however, they are in agreement with the proposed mechanism of auto-regulation of KRAB-ZFP-encoding genes (O'Geen et al. 2007). According to this model,

KRAB-ZFPs can self-inhibit their expression through interaction with the TRIM28 corepressor complex that needs to interact with HP1 for some, but not all of its functions (O'Geen et al. 2007; Herzog et al. 2011). Therefore, we hypothesized that in HP1-TKO livers, KRAB-ZPF-encoding genes are over-expressed because of the loss of TRIM28 activity as a consequence of the absence of HP1 proteins and that, for the same reason, KRAB-ZFPs cannot repress their ERV targets.

HP1 proteins are necessary for TRIM28 activity in liver

To investigate the relationship between HP1, KRAB-ZFPs, TRIM28 and ERVs in liver, RNA-seq, RT-qPCR and western blot assays were used to analyze the effect of HP1 loss on TRIM28 expression in liver. TRIM28 expression was not significantly different in HP1-TKO and control livers (Fig. 5A-B). However, chromatin fractionation showed that TRIM28 association with chromatin was reduced in HP1-TKO compared with control samples, indicating that HP1 proteins are essential for TRIM28 recruitment to and/or stabilization at chromatin (Fig. 5C). Then, the role of the TRIM28-HP1 interaction in liver was investigated using the Alb-Cre mouse model in which a mutated TRIM28 protein that cannot interact with HP1 (T28HP1box) is replacing TRIM28 (Herzog et al. 2011). As control, our previously described mouse model in which TRIM28 is specifically inactivated in the liver (T28KO) was used (Herzog et al. 2011). As expected, TRIM28 expression was strongly decreased in T28KO livers, whereas it was only decreased by about two-fold in T28HP1box livers (this mutation is present only on one *Trim28* allele, and the other one is inactivated) (Fig. 5D). The level of the three HP1 proteins was not affected in these mouse strains. RT-qPCR analysis showed that several HP1-dependent genes that were either downregulated (*Nox4* and *Cypc29*) or upregulated (*Ifit2* and *Rsl1*) in HP1-TKO liver samples were not affected in T28HP1box and T28KO livers (Fig. 5E). Conversely, *Cyp2b10* and the KRAB-ZFP-encoding genes *Zfp345* and *Zfp445* (all overexpressed in HP1-TKO liver) were upregulated also in

T28HP1box and T28KO livers (Fig. 5E). The higher expression level of *Zfp345* in T28HP1box than in T28KO livers strongly suggested a dominant negative role of T28HP1box on its expression. Altogether, these data demonstrated that HP1 proteins regulate gene expression through TRIM28-dependent and -independent mechanisms and that, with the exception of *Rsl1,* all other tested HP1-dependent KRAB-ZFP-encoding genes were regulated by a mechanism that requires HP1, TRIM28 and their interaction. To test whether the HP1-dependent ERV-associated genes also required TRIM28, the expression of *Mbd1* and *Bglap3* was assessed in T28KO and T28HP1box livers. Like in HP1-TKO livers, they were overexpressed in both samples, although *Bglap3* expression level was much lower in the TRIM28 mutants than in HP1-TKO livers (Fig. 5F).

HP1 proteins prevent tumor development in liver

Although apparently healthy, young and middle-aged HP1-TKO mice displayed alterations in heterochromatin organization and in the expression of liver homeostasis genes as well as ERV reactivation, all features that could promote tumor development (Scarfò et al. 2016). In agreement, analysis of old mice (>44 weeks of age) indicated that although HP1-TKO animals (n=17) were morphologically indistinguishable from control littermates (n=67), 76.4% of them had liver tumors compared with 6.4% of controls (Fig. 6A). No difference was observed in the percentage of mice with tumors between HP1-TKO females and males (72.7%, n=11, and 83.3%, n=6, respectively). The number and size of tumors were very variable among animals (Fig. 6B), suggesting that besides HP1 absence, other factors were involved in tumor development. Verification of the excision of the *Cbx*1 (HP1β) and *Cbx*3 (HP1γ) genes in tumor and healthy liver tissues indicated that tumors originated from HP1-TKO hepatocytes (Supplementary Fig. 3A). Histological analysis of paraffin-embedded liver tissue sections revealed that most old male (M-TKO) and female (F-TKO) HP1-TKO animals developed tumor nodules that could easily be distinguished from the rest of the liver

parenchyma (Fig. 6C). These nodules were characterized by the presence of well-differentiated hepatocytes but without their specific trabecular organization, and thus, were identified as typical hepatocellular carcinoma (HCC). Moreover, RT-qPCR analysis of the expression of α-fetoprotein (*Afp*), a marker of human HCC, in control and in normal (TKON) and tumor (TKOT) HP1-TKO liver samples showed that *Afp* was strongly overexpressed exclusively in the tumor tissue of three of the five tested tumors (Supplementary Figure 3B). Analysis of cell proliferation (Ki67), apoptosis (activated caspase 3) and global response to DNA damage (γH2AX) by IHC on TMA of paraffin-embedded liver sections from old mice showed a two-fold increase only of cell proliferation in both the tumor (TKOT) and non-tumor (TKON) parts of HP1-TKO liver samples compared with control parts whereas no change was detected in the number of apoptotic-positive cells nor of positive γH2AX cells (Supplementary Fig. 3B). These data indicated that whereas in old controls hepatocytes were mostly quiescent, cell proliferation was increased in old HP1-TKO animals that are more prone to tumor development.

Similarly, T28KO and T28HP1box mice older than 42 weeks of age developed more frequently tumors in livers than controls, although at a lower rate than HP1-TKO animals (38.5% and 35.7% for T28KO and T28HP1box males and 26.3% and 31.2% for T28KO and T28HP1box females, respectively, Fig. 6D-E) strengthening the mechanistic link between HP1 proteins and TRIM28 for liver tumor prevention.

Finally, expression analysis of the ERV-associated *Mbd1* and *Bglap3* in old animals (Fig. 6F) showed that compared with controls, both genes were strongly upregulated in both normal (TKON) and tumor (TKOT) liver samples from old HP1-TKO animals. However, and in contrast with what observed in young and middle-aged animals, *Mbd1* was no longer overexpressed in the liver (normal and tumor samples) of old TRIM28 mutant mice, whereas *Bglap3* was still upregulated only in T28KO livers (Fig. 6G). This suggests that TRIM28 is necessary in old animals to maintain low expression of only a subset of its target genes and that its association with HP1 is not required for this function.

DISCUSSION

In this study, we used the Cre-LoxP system in which the recombinase Cre expression was induced by the albumin promoter to inactivate the three chromatin-associated HP1 proteins in hepatocytes as soon as they acquired their identity during mouse development (Weisend et al. 2009). To our knowledge, this is the first demonstration that some cells can develop, proliferate and function in the complete absence of all three HP1 proteins. Conversely, HP1 proteins are essential for preventing liver tumor development.

The finding that in the mouse, the three HP1 proteins are not essential for liver function is in contrast with previous studies showing their fundamental functions during embryonic development in various species, such as *Drosophila* (Eissenberg et al. 1992), C. *elegans* (Schott et al. 2006) and the mouse (our unpublished data). This suggests that HP1 functional requirement is inversely correlated with the level of cell differentiation. This is also in apparent contrast with the reported key HP1 roles in nuclear functions and chromatin organization. One can hypothesize that liver chromatin organization and functions are highly specific and mostly independent of HP1 and/or that some compensatory mechanisms take place specifically in mouse liver (Eissenberg and Elgin 2014; Kwon and Workman 2011; Nishibuchi and Nakayama 2014). In favor of the hypothesis of a specific liver chromatin organization, it is important to note that liver is the only tissue that regenerate upon stress (e.g., partial hepatectomy) essentially through the re-entry into the cell cycle of quiescent and fully differentiated hepatocytes (Fausto et al. 2006; Kurinna and Barton 2011), and not via stem cell proliferation, like in other tissues. This specific ability of differentiated hepatocytes to enter/exit quiescence could rely on a peculiar loose chromatin organization that might be less sensitive to HP1 absence compared with other cell types.

Although the exact mechanisms whereby HP1 proteins prevent tumor development are not known yet, our study highlighted major HP1 roles in heterochromatin organization, gene expression and ERV silencing the alteration of which could contribute to liver hepatocytes transformation. Specifically, HP1 loss was accompanied by a drastic reduction of the two heterochromatin marks H3K9me3 and H4K20me3, without significant disorganization of chromocenters that are normally characterized by an enrichment in H3K9me3 and HP1 (Fig. 2). However, these DAPI-dense structures were partially re-localized towards the nucleus periphery, suggesting a subtle re-organization of the heterochromatic compartment. Moreover, and differently from what reported upon loss of H3K9me3 induced by inactivation of the histone methyltransferases SUV39H1 and SUV39H2 (Lehnertz et al. 2003; Velazquez Camacho et al. 2017), the loss of H3K9me3 in HP1-TKO hepatocytes did not result in the overexpression of major satellite repeats, but rather in a slight downregulation. This observation is in line with the finding, again in contrast with *Suv39h1/2* gene ablation, that H3K9me2 was not decreased in HP1-TKO mice, strongly supporting the conclusion that this histone modification is sufficient to keep major satellite sequences silent (Fig. 2D). The loss of H3K9me3 in HP1-TKO mice might not be the key determinant of tumorigenesis because it was reported that SUV39H1 overexpression is associated with HCC development (Fan et al. 2013). Moreover, HCC induced by a methyl-free diet also is characterized by elevated SUV39H1 expression and increased H3K9me3 and reduced H4K29me3 deposition. Decreased H4K29me3 was also observed in HP1-TKO mice and might be involved in tumorigenesis (Pogribny et al. 2006). Indeed, H4K20me3 is essential for genome integrity and proper timing of heterochromatin replication (Brustel et al. 2017; Jørgensen et al. 2013). Further investigations are required to determine which, if any, alteration of heterochromatin organization induced by the lack of the three HP1 proteins is involved in tumorigenesis.

HP1 ablation also led to the deregulation (both up and down-regulation) of many genes, strongly suggesting that the three HP1 proteins are involved in both repression and

activation of gene expression, as reported by others (Lee et al. 2013; Piacentini et al. 2009; Vakoc et al. 2005). One of the most striking results in the present study was the enrichment among the upregulated genes of genes encoding members of the KRAB-ZFP family of transcriptional co-repressors. Very little functional information is available about most of these transcription factors, but transposable elements of the ERV family are one of their main known targets (Jacobs et al. 2014; Wolf et al. 2015; Yang et al. 2017). These mobile genetic elements constitute a threat for the genome stability and/or gene expression because of their ability to insert at any genomic location. However and paradoxically, increasing evidence suggests that they have been coopted to serve as regulatory sequences in the host genome (Thompson et al. 2016). Thus, an important challenge for the genome is to keep all these elements silent and unable to get transposed. ERV are repressed by the KRAB-ZFP/TRIM28 complex, and HP1 proteins are involved in the repression activity of this complex; however, HP1 proteins are dispensable for ERV silencing in ES cells (Maksakova et al. 2011). Here, we found that the three HP1 proteins, most likely through regulation of the KRAB/TRIM28 complex, are involved in silencing of specific ERVs in liver. Although it is not known why silencing of some ERVs is HP1-dependent, our data strongly suggest that the reactivation of some of these ERVs induce the overexpression of genes in their vicinity either by behaving as enhancer-like elements as proposed by others(Herquel et al. 2013; Bojkowska et al. 2012b), for instance in the case of the *Zfp445*, *Fbwx19* and *Obp2a* genes, or as alternative promoters (e.g., for the *Mbd1* and *Bglap3* genes). Interestingly, inactivation of the nuclear receptor corepressor TRIM24 leads to *Mbd1, Zfp445, Obp2a* overexpression, whereas inactivation of the KRAB-ZFP corepressor TRIM28 causes overexpression of *Bglap3 and Fbxw19* (Ecco et al. 2016; Herquel et al. 2013). Altogether, these data strongly suggest that HP1 acts upstream of these two corepressors, a conclusion in line with our previous observation that TRIM24 and TRIM28 can be found in the same complex in liver (Herquel et al. 2011), and with our hypothesis that HP1 regulates TRIM28 activity in liver. Therefore, ERV overexpression might play a key role in tumorigenesis induced by the absence of the three HP1 proteins, as suggested by others (Scarfò et al. 2016).

In conclusion, we showed here that surprisingly, hepatocytes can survive and function normally in the concomitant absence of HP1α, β and γ, despite the loss of all heterochromatin histone marks, and that the three HP1 proteins are essential to prevent tumor development in liver.

MATERIALS AND METHODS

Mouse models.

The Cbx5KO, T28KO (TRIM28KO) and T28HP1box (TRIM28-L2/HP1box) mouse strains were described previously (Allan et al. 2012; Herzog et al. 2011; Cammas et al. 2000). Exons 2 to 4 within the *Cbx1* gene (HP1β), and exon 3 within the *Cbx3* gene (HP1γ) were surrounded by LoxP sites. Excision of the floxed exons exclusively in hepatocytes by using mice that express the Cre recombinase under the control of the albumin promoter (Alb-Cre mice, (Postic et al. 1999)) led to the removal of the starting ATG codon of the two genes, as well as to a frameshift within the CSD-encoding sequence of *Cbx1* and the CD-encoding sequence of *Cbx3. Cbx5,* the gene encoding HP1α, was inactivated in all body cells by removing exon 3 using the Cre recombinase under the control of the cytomegalovirus (CMV) promoter, as described previously (Cbx5KO mice) (Allan et al. 2012). *Cbx5*+/- animals were then crossed with *Cbx3*L2/L2 and Cbx1L2/L2 animals to generate mice in which all three proteins can be depleted in tissues upon expression of the Cre recombinase. *Cbx5*+/-; *Cbx3*L2/L2; Cbx1L2/L2 were crossed with Alb-Cre transgenic mice to produce *Cbx5*+/-; *Cbx3*L2/+; Cbx1L2/+; Alb-Cre mice that were intercrossed to finally produce HP1-TKO mice and their controls. TRIM28L2/HP1box were crossed with Alb-Cre transgenic mice to produce mice that express TRIM28HP1box as the only TRIM28 protein in hepatocytes (TRIM28-liverL-/HP1box, called T28HP1box mice in this article).

For each experiment, experimental and control mice were age-matched and whenever possible were littermates. A minimum of three animals of each genotype were used for each experiment. This number was deemed sufficiently appropriate to account for normal variation, as determined from previous studies. The number of animals used for each experiment is indicated in the figure legends. No statistical method was used to predetermine sample size.

Mice were housed in a pathogen-free barrier facility, and experiments were approved by the national ethics committee for animal warfare (n°CEEA-36).

Antibodies/oligonucleotides

The antibodies used in this study were: the rabbit anti-TRIM28 polyclonal antibody PF64, raised against amino acids 141–155 of TRIM28[64]; the anti-HP1α, anti-HP1β and anti-HP1γ monoclonal antibodies 2HP2G9, 1MOD1A9, and 2MOD1G6[65], respectively. Anti-Casp3A (9661, Cell Signaling); anti-γH2AX (Ab11174, Abcam), anti-Ki67 (M3064, Spring Bioscience). Oligonucleotides are described in Supplementary Table 10.

Tissue processing for histology.

For fresh frozen tissues, 3mm sections of the liver large lobe were embedded in the OCT compound (TissueTek) following standard protocols, and 18μm-thick sections were cut using a Leica CM1850 cryostat and stored at −80 °C.

For paraffin-embedded tissues, 3mm sections of the liver large lobe were fixed in 4% neutral-buffered formalin (VWR Chemicals) at room temperature (RT) overnight, and stored in 70% ethanol at 4°C. Fixed tissues were processed using standard protocols and embedded in paraffin wax. Three-µm-thick sections were cut using a Thermo Scientific Microm HM325 microtome, dried at 37 °C overnight and stored at 4 °C.

Immunofluorescence analysis.

Cryosections were fixed in formaldehyde (2%) at RT for 15min, and then air dried at RT for 20min. Sections were rinsed in PBS (3 x 15min) and incubated in 5% BSA/PBS/0.3% Triton X-100 at RT for 30min to block non-specific antibody binding. Sections were the incubated with primary antibodies diluted in 1% BSA/PBS/0.3% Triton X-100 at 4 °C overnight, or at RT for 1 h. Sections were then washed in PBS/0.1% Triton X-100 (3 × 5 min) and incubated with the appropriate secondary antibody [goat-anti-rabbit Alexa Fluor 488 (Molecular Probes, 1:800), goat-anti-mouse Alexa Fluor 568 (Molecular Probes, 1:800)] diluted in 1% BSA/PBS/0.3% Triton X-100 at RT for 1h. After three washes (5min/each) in PBS/0.1% Triton X-100, sections were washed in water for 5 min before mounting with VECTASHIELD

mounting medium (Vector Laboratories) with 4',6-Diamidino-2-Phenylindole, Dihydrochloride (DAPI). Sections were dried at RT overnight, and then kept at 4°C before image acquisition with a Zeiss Apotome2 microscope and analysis using ImageJ.

Immunohistochemistry.

Paraffin-embedded liver sections were processed for routine hematoxylin, eosin and Safran or reticulin staining. For immunohistochemistry, sections were washed in PBS/1% Triton X-100 at RT (3 x 30 min) and incubated in blocking solution (PBS/1% Triton X-100/10% fetal calf serum/0.2% sodium azide) at RT twice for 1h, followed by incubation in 3% H_2O_2 in blocking solution at 4 °C overnight. This was followed by two washes of 15 min/each in blocking solution, and incubation with primary antibodies at 4 °C overnight. Sections were washed in blocking solution (3 x 1h), and then in PBS/1% Triton X-100 (3 x 10min). The secondary antibody was diluted in blocking solution (without sodium azide) and added at RT for 1h. Sections were then washed in PBS (3 × 1 h) before mounting with VECTASHIELD mounting medium with DAPI. Images were acquired with a Zeiss Apotome2 microscope and processed using ImageJ.

RNA extraction and RT-qPCR assays

RNA was isolated from liver samples using TRIzol, according to the manufacturer's recommendations (Life technologies). 2µg of total RNA was incubated with 2U of DNase 1 at 37°C for 30min. For reverse transcription, a mixture containing 2µg of DNA-free total RNA, 0.125µg of random primers and 0.25µg of oligodT was denatured at 70°C for 10min, and then incubated with 1U Superscript III (Invitrogen) at 50°C for 1h. 1/100 of this reaction was used for real-time qPCR amplification using SYBR Green I (SYBR Green SuperMix, Quanta).

RNA-seq

Total RNA from liver samples from 7-week-old control and HP1-KO mice was used for library preparation using the Illumina TruSeq Stranded mRNA Sample Preparation kit.

Polyadenylated RNA was purified using magnetic oligo(dT) beads and then fragmented into small pieces using divalent cations at elevated temperature. The cleaved RNA fragments were copied into first-strand cDNA using reverse transcriptase and random primers in the presence of actinomycin D. Second-strand cDNA synthesis was performed using dUTP, instead of dTTP, resulting in blunt double-stranded cDNA fragments. A single ‘A’ nucleotide was added to the 3’ ends of the blunt DNA fragments using a Klenow fragment (3' to 5'exo minus). The cDNA fragments were ligated to double-stranded TruSeq Universal adapters using T4 DNA Ligase. The ligated products were enriched by PCR amplification (98°C for 30sec, followed by 15 cycles of 98°C for 10sec, 60°C for 30sec, and 72°C for 30sec; finally, 72°C for 5min). Then, the excess of PCR primers was removed by purification using AMPure XP beads (Agencourt Biosciences Corporation). The quality and quantity of the final cDNA libraries were checked using a Fragment Analyzer (AATI) and the KAPA Library Quantification Kit (Roche), respectively. Libraries were equimolarly pooled and sequenced (50nt single read per lane) on a Hiseq2500 apparatus, according to the manufacturer’s instructions. Image analysis and base calling were performed using the Illumina HiSeq Control software and the Illumina RTA software. Reads not mapping to rRNA sequences were mapped onto the mouse genome mm10 assembly using the Tophat mapper (v2.0.10 58) and the Bowtie2 (v2.1.0) aligner. Gene expression was quantified from uniquely aligned reads using HTSeq v0.5.4p3 59 and gene annotations from the Ensembl release 75.

Statistical analyses were performed using the method previously described (Love et al. 2014) implemented in the DESeq2 Bioconductor library (v1.0.19), taking into account the batch effect. Adjustment for multiple testing was performed with the Hochberg and Benjamini method (Hochberg and Benjamini 1990).

For repeat analysis, alignment positions were compared with repeats annotated in UCSC with RepeatMasker (rmsk table from mm10) and overlaps were kept relative to the strand. Among the multiple mapped reads, only those mapping to the same repeat type were kept. Repeat types that were significantly different between conditions were identified with

DESeq2 v1.0.19. Repeats found in exons were removed from the analysis because it was not possible to discriminate between differential gene and repeat expression.

Data are available at GEO (accession number: GSE119244).

Extraction of mouse liver nuclei

Adult male mice were euthanized, and their livers removed and placed on ice. After dissection of the liver lobes and removal of the connective tissue and blood vessels, approximatively 100 µg of liver tissue was washed in ice-cold homogenizing buffer (HB, 0.32M sucrose, 5mM $MgCl_2$, 60mM KCl, 15mM NaCl, 0.1mM EGTA, 15mM Tris-HCl pH 7.4), minced with scissors, and homogenized with 7 ml of HB using a 15 ml Wheaton Dounce homogenizer and 20 strokes of the loose B pestle. Unless otherwise indicated, all subsequent steps were performed at 4°C. Homogenates were filtered through 100 µM layers of gauze, taken to 7 ml with HB and centrifuged in 15 ml Corning tubes at 6000 g for 10min. After discarding the supernatant, pellets were gently resuspended in the same tube with 2 ml of HB and 2 ml of nuclear extraction buffer (HB plus 0.4% Nonidet P-40) and incubated on ice for 10min. The mixtures were centrifuged (10.000 g for 10 min) in two tubes in which 8ml of separating buffer (1.2M sucrose, 5mM $MgCl_2$, 60mM KCl, 15mM NaCl, 0.1mM EGTA, 15mM Tris-HCl pH 7.4) was added. Pellets were resuspended in 1.0 ml of 0.25M sucrose and 1mM $MgCl_2$, and transferred to a 1.5 ml Eppendorf tube. Nuclei were collected by centrifugation at 700 g at 4 °C for 10 min and stored at -70°C until use.

Subcellular fractionation

After dissection of liver lobes, approximatively 150 µg of liver tissue was washed in ice-cold HB, minced with scissors and homogenized in 7 ml of HB using a 15 ml Wheaton Dounce homogenizer and 20 strokes of the loose B pestle. Homogenates were filtered through 100 µM layers of gauze, taken to 7 ml with HB and centrifuged at 6000 g in 15 ml Corning tubes

for 10min. After discarding the supernatants, pellets were gently resuspended in 400 µl of hypotonic buffer (10mM HEPES-NaOH, pH 7.5, 10mM KCl, 1.5mM $MgCl_2$, 0.34M sucrose, 10% glycerol, 0.15% Nonidet P-40, 50 mM APMSF, 10 mg/liter leupeptin, 3 mg/liter pepstatin, 50mM NaF, 2mM Na_3VO_4, and 25mM glycerophosphate), and kept at 4°C for 9min. Cells were then resuspended by pipetting. A 100µl-aliquot of each sample was collected (whole-cell extract), and the rest of each sample was centrifuged at 800 g at 4°C for 10min. Supernatants were centrifuged again at 20.000 g at 4°C for 10min and collected (cytosolic fraction). The nuclear pellets were washed twice in hypotonic buffer, resuspended in 200 µl of nuclear extract buffer (420mM NaCl, 20mM HEPES-NaOH, pH 7.5, 20% glycerol, 2mM $MgCl_2$, 0.2mM EDTA, 0.2% Nonidet P-40) and kept at 4°C for 1h, and then centrifuged at 20800g at 4°C for 45min. Supernatants were collected (nuclear fraction). The insoluble chromatin pellets were resuspended in 150 µl of radio immunoprecipitation assay (RIPA) buffer, briefly sonicated to solubilize the chromatin fraction, and stored at -80°C until use.

Chromatin immunoprecipitation (ChIP) experiments

ChIP assays were performed as described previously (Saksouk et al. 2014). Briefly, 150 µg of liver tissue was washed in ice-cold HB, minced with scissors and homogenized with 7 ml of HB using a 15 ml Wheaton Dounce homogenizer and 20 strokes of the loose B pestle. All subsequent steps were performed at 4 °C. Homogenates were filtered through 100 µM layers of gauze and chromatin crosslinked with 1% formaldehyde. Chromatin was extracted in lysis buffer (50mM Tris-HCl pH 8, 10mM EDTA, 0.5% SDS, 5mM sodium butyrate, and 10µM zinc chloride) and then sheared by sonication (Active Motif) on ice to an average length of 500bp. After pre-clearing with a mix of protein A/G Dynabeads (for 1h), 100µg of chromatin was used for immunoprecipitation with antibodies against histone H3K9me3 (Active Motif #39161) and H3 (C terminus, Abcam #1791). After overnight incubation, beads were extensively washed and immunoprecipitates were eluted in buffer E (50mM sodium bicarbonate/1%

SDS). Cross-links were reversed at 65°C overnight. The following day, samples were incubated with proteinase K, and DNA was extracted using phenol/chloroform.

Statistics and reproducibility.

The Microsoft Excel software was used for statistical analyses; the used statistical tests, number of independent experiments, and P-values are listed in the individual figure legends. All experiments were repeated at least twice unless otherwise stated.

ACKNOWLEDGMENTS:

We thank P. Chambon, C. Sardet, T. Forné, D.Fisher, E. Julien and C. Grimaud for helpful discussions and critical reading of the manuscript. We thank F. Bernex and L. LeCam, C. Keime and B. Jost for fruitful discussions. We thank L. Papon, H. Fontaine and C. Bonhomme for technical assistance and M. Oulad-Abdelghani and the IGBMC for the anti-HP1 and TRIM28 antibodies. We also thank the RHEM technical facility and particularly J. Simony for histological analysis and the IGBMC/ICS transgenic and animal facility for the initial establishment of the HP1 and TRIM28 mouse models. We thank C. Vincent and the IRCM animal core facility for the day to day care of the animal models. Finally, we thank S. Chamroeun for counting positive cells on TMA. We acknowledge the imaging facility MRI, member of the national infrastructure France-BioImaging and supported by the French National Research Agency (ANR-10-INBS-04, «Investments for the future»).

This work was supported by funds from the Centre National de la Recherche Scientifique (CNRS), the Institut National de la Santé et de la Recherche Médicale (INSERM), the University of Montpellier and the Institut regional de Cancérologie de Montpellier (ICM). SH was funded by an Erasmus PhD fellowship. We also thank the Ministry of Education, Science and Technology of the Republic of Kosovo for a scholarships to support SH. FC was supported by grants from ANR (ANR 2009 BLAN 021 91; ANR-16CE15-0018-03), INCa (PLBIO13-146), ARC (PJA20131200357), and La ligue Régionale contre le Cancer (128-R13021FF-RAB13006FFA). Sequencing was performed by the MGX facility. Montpellier, France.

AUTHORS' CONTRIBUTIONS:

NS and SH performed the analysis of mice and interpreted the data. MP and CB made the libraries, generated and analyzed the RNA-seq data. AZ performed most of the RT-qPCR experiments. NP supervised the histological core facility and JYN performed the TMA. LK performed the pathological analysis of histological sections. EF performed some of the RT-qPCR analyses. FC designed, analyzed and interpreted the data and wrote the manuscript with input from all co-authors.

REFERENCES

Abe K, Naruse C, Kato T, Nishiuchi T, Saitou M, Asano M. 2011. Loss of heterochromatin protein 1 gamma reduces the number of primordial germ cells via impaired cell cycle progression in mice. *Biol Reprod* **85**: 1013–1024.

Allan RS, Zueva E, Cammas F, Schreiber HA, Masson V, Belz GT, Roche D, Maison C, Quivy J-P, Almouzni G, et al. 2012. An epigenetic silencing pathway controlling T helper 2 cell lineage commitment. *Nature* **487**: 249–253.

Aucott R, Bullwinkel J, Yu Y, Shi W, Billur M, Brown JP, Menzel U, Kioussis D, Wang G, Reisert I, et al. 2008. HP1-beta is required for development of the cerebral neocortex and neuromuscular junctions. *J Cell Biol* **183**: 597–606.

Bhattacharyya S, Sinha K, Sil PC. 2014. Cytochrome P450s: mechanisms and biological implications in drug metabolism and its interaction with oxidative stress. *Curr Drug Metab* **15**: 719–742.

Bojkowska K, Aloisio F, Cassano M, Kapopoulou A, Santoni de Sio F, Zangger N, Offner S, Cartoni C, Thomas C, Quenneville S, et al. 2012a. Liver-specific ablation of Krüppel-associated box-associated protein 1 in mice leads to male-predominant hepatosteatosis and development of liver adenoma. *Hepatology* **56**: 1279–1290.

Bojkowska K, Aloisio F, Cassano M, Kapopoulou A, Santoni de Sio F, Zangger N, Offner S, Cartoni C, Thomas C, Quenneville S, et al. 2012b. Liver-specific ablation of Krüppel-associated box-associated protein 1 in mice leads to male-predominant hepatosteatosis and development of liver adenoma. *Hepatology* **56**: 1279–1290.

Bosch-Presegué L, Raurell-Vila H, Thackray JK, González J, Casal C, Kane-Goldsmith N, Vizoso M, Brown JP, Gómez A, Ausió J, et al. 2017. Mammalian HP1 Isoforms Have

Specific Roles in Heterochromatin Structure and Organization. *Cell Rep* **21**: 2048–2057.

Brown JP, Bullwinkel J, Baron-Lühr B, Billur M, Schneider P, Winking H, Singh PB. 2010. HP1gamma function is required for male germ cell survival and spermatogenesis. *Epigenetics Chromatin* **3**: 9.

Brustel J, Kirstein N, Izard F, Grimaud C, Prorok P, Cayrou C, Schotta G, Abdelsamie AF, Déjardin J, Méchali M, et al. 2017. Histone H4K20 tri-methylation at late-firing origins ensures timely heterochromatin replication. *EMBO J* **36**: 2726–2741.

Cammas F, Mark M, Dollé P, Dierich A, Chambon P, Losson R. 2000. Mice lacking the transcriptional corepressor TIF1beta are defective in early postimplantation development. *Development* **127**: 2955–2963.

Cichoż-Lach H, Michalak A. 2014. Oxidative stress as a crucial factor in liver diseases. *World J Gastroenterol* **20**: 8082–8091.

Dialynas GK, Vitalini MW, Wallrath LL. 2008. Linking Heterochromatin Protein 1 (HP1) to cancer progression. *Mutat Res* **647**: 13–20.

Dinant C, Luijsterburg MS. 2009. The emerging role of HP1 in the DNA damage response. *Mol Cell Biol* **29**: 6335–6340.

Ecco G, Cassano M, Kauzlaric A, Duc J, Coluccio A, Offner S, Imbeault M, Rowe HM, Turelli P, Trono D. 2016. Transposable Elements and Their KRAB-ZFP Controllers Regulate Gene Expression in Adult Tissues. *Dev Cell* **36**: 611–623.

Eissenberg JC, Elgin SCR. 2014. HP1a: a structural chromosomal protein regulating transcription. *Trends Genet* **30**: 103–110.

Eissenberg JC, Morris GD, Reuter G, Hartnett T. 1992. The heterochromatin-associated protein HP-1 is an essential protein in Drosophila with dosage-dependent effects on position-effect variegation. *Genetics* **131**: 345–352.

Fan DN-Y, Tsang FH-C, Tam AH-K, Au SL-K, Wong CC-L, Wei L, Lee JM-F, He X, Ng IO-L, Wong C-M. 2013. Histone lysine methyltransferase, suppressor of variegation 3-9 homolog 1, promotes hepatocellular carcinoma progression and is negatively regulated by microRNA-125b. *Hepatology* **57**: 637–647.

Fanti L, Pimpinelli S. 2008. HP1: a functionally multifaceted protein. *Curr Opin Genet Dev* **18**: 169–174.

Fausto N, Campbell JS, Riehle KJ. 2006. Liver regeneration. *Hepatology* **43**: S45-53.

Hardy T, Mann DA. 2016. Epigenetics in liver disease: from biology to therapeutics. *Gut* **65**: 1895–1905.

Herquel B, Ouararhni K, Khetchoumian K, Ignat M, Teletin M, Mark M, Béchade G, Van Dorsselaer A, Sanglier-Cianférani S, Hamiche A, et al. 2011. Transcription cofactors TRIM24, TRIM28, and TRIM33 associate to form regulatory complexes that suppress murine hepatocellular carcinoma. *Proc Natl Acad Sci USA* **108**: 8212–8217.

Herquel B, Ouararhni K, Martianov I, Le Gras S, Ye T, Keime C, Lerouge T, Jost B, Cammas F, Losson R, et al. 2013. Trim24-repressed VL30 retrotransposons regulate gene expression by producing noncoding RNA. *Nat Struct Mol Biol* **20**: 339–346.

Herzog M, Wendling O, Guillou F, Chambon P, Mark M, Losson R, Cammas F. 2011. TIF1β association with HP1 is essential for post-gastrulation development, but not for Sertoli cell functions during spermatogenesis. *Dev Biol* **350**: 548–558.

Hochberg Y, Benjamini Y. 1990. More powerful procedures for multiple significance testing. *Stat Med* **9**: 811–818.

Jacobs FMJ, Greenberg D, Nguyen N, Haeussler M, Ewing AD, Katzman S, Paten B, Salama SR, Haussler D. 2014. An evolutionary arms race between KRAB zinc-finger genes ZNF91/93 and SVA/L1 retrotransposons. *Nature* **516**: 242–245.

James TC, Elgin SC. 1986. Identification of a nonhistone chromosomal protein associated with heterochromatin in Drosophila melanogaster and its gene. *Mol Cell Biol* **6**: 3862–3872.

Janssen A, Colmenares SU, Karpen GH. 2018a. Heterochromatin: Guardian of the Genome. *Annu Rev Cell Dev Biol*.

Janssen A, Colmenares SU, Karpen GH. 2018b. Heterochromatin: Guardian of the Genome. *Annu Rev Cell Dev Biol*.

Jenuwein T, Allis CD. 2001. Translating the histone code. *Science* **293**: 1074–1080.

Jørgensen S, Schotta G, Sørensen CS. 2013. Histone H4 lysine 20 methylation: key player in epigenetic regulation of genomic integrity. *Nucleic Acids Res* **41**: 2797–2806.

Khetchoumian K, Teletin M, Tisserand J, Mark M, Herquel B, Ignat M, Zucman-Rossi J, Cammas F, Lerouge T, Thibault C, et al. 2007. Loss of Trim24 (Tif1alpha) gene function confers oncogenic activity to retinoic acid receptor alpha. *Nat Genet* **39**: 1500–1506.

Koschmann C, Nunez FJ, Mendez F, Brosnan-Cashman JA, Meeker AK, Lowenstein PR, Castro MG. 2017. Mutated Chromatin Regulatory Factors as Tumor Drivers in Cancer. *Cancer Res* **77**: 227–233.

Kuo LJ, Yang L-X. 2008. Gamma-H2AX - a novel biomarker for DNA double-strand breaks. *In Vivo* **22**: 305–309.

Kurinna S, Barton MC. 2011. Cascades of transcription regulation during liver regeneration. *Int J Biochem Cell Biol* **43**: 189–197.

Kwon SH, Workman JL. 2011. The changing faces of HP1: From heterochromatin formation and gene silencing to euchromatic gene expression: HP1 acts as a positive regulator of transcription. *Bioessays* **33**: 280–289.

Lee DH, Li Y, Shin D-H, Yi SA, Bang S-Y, Park EK, Han J-W, Kwon SH. 2013. DNA microarray profiling of genes differentially regulated by three heterochromatin protein 1 (HP1) homologs in Drosophila. *Biochem Biophys Res Commun* **434**: 820–828.

Lehnertz B, Ueda Y, Derijck AAHA, Braunschweig U, Perez-Burgos L, Kubicek S, Chen T, Li E, Jenuwein T, Peters AHFM. 2003. Suv39h-mediated histone H3 lysine 9 methylation directs DNA methylation to major satellite repeats at pericentric heterochromatin. *Curr Biol* **13**: 1192–1200.

Lomberk G, Wallrath L, Urrutia R. 2006. The Heterochromatin Protein 1 family. *Genome Biol* **7**: 228.

Love MI, Huber W, Anders S. 2014. Moderated estimation of fold change and dispersion for RNA-seq data with DESeq2. *Genome Biol* **15**: 550.

Maksakova IA, Goyal P, Bullwinkel J, Brown JP, Bilenky M, Mager DL, Singh PB, Lorincz MC. 2011. H3K9me3-binding proteins are dispensable for SETDB1/H3K9me3-dependent retroviral silencing. *Epigenetics Chromatin* **4**: 12.

Martens JHA, O'Sullivan RJ, Braunschweig U, Opravil S, Radolf M, Steinlein P, Jenuwein T. 2005. The profile of repeat-associated histone lysine methylation states in the mouse epigenome. *EMBO J* **24**: 800–812.

Mirabella AC, Foster BM, Bartke T. 2016. Chromatin deregulation in disease. *Chromosoma* **125**: 75–93.

Nishibuchi G, Nakayama J. 2014. Biochemical and structural properties of heterochromatin protein 1: understanding its role in chromatin assembly. *J Biochem* **156**: 11–20.

O'Geen H, Squazzo SL, Iyengar S, Blahnik K, Rinn JL, Chang HY, Green R, Farnham PJ. 2007. Genome-wide analysis of KAP1 binding suggests autoregulation of KRAB-ZNFs. *PLoS Genet* **3**: e89.

Paik Y-H, Kim J, Aoyama T, De Minicis S, Bataller R, Brenner DA. 2014. Role of NADPH oxidases in liver fibrosis. *Antioxid Redox Signal* **20**: 2854–2872.

Park JW, Reed JR, Brignac-Huber LM, Backes WL. 2014. Cytochrome P450 system proteins reside in different regions of the endoplasmic reticulum. *Biochem J* **464**: 241–249.

Piacentini L, Fanti L, Negri R, Del Vescovo V, Fatica A, Altieri F, Pimpinelli S. 2009. Heterochromatin protein 1 (HP1a) positively regulates euchromatic gene expression through RNA transcript association and interaction with hnRNPs in Drosophila. *PLoS Genet* **5**: e1000670.

Pogribny IP, Ross SA, Tryndyak VP, Pogribna M, Poirier LA, Karpinets TV. 2006. Histone H3 lysine 9 and H4 lysine 20 trimethylation and the expression of Suv4-20h2 and Suv-39h1 histone methyltransferases in hepatocarcinogenesis induced by methyl deficiency in rats. *Carcinogenesis* **27**: 1180–1186.

Postic C, Shiota M, Niswender KD, Jetton TL, Chen Y, Moates JM, Shelton KD, Lindner J, Cherrington AD, Magnuson MA. 1999. Dual roles for glucokinase in glucose homeostasis as determined by liver and pancreatic beta cell-specific gene knock-outs using Cre recombinase. *J Biol Chem* **274**: 305–315.

Saksouk N, Barth TK, Ziegler-Birling C, Olova N, Nowak A, Rey E, Mateos-Langerak J, Urbach S, Reik W, Torres-Padilla M-E, et al. 2014. Redundant mechanisms to form

silent chromatin at pericentromeric regions rely on BEND3 and DNA methylation. *Mol Cell* **56**: 580–594.

Scarfò I, Pellegrino E, Mereu E, Inghirami G, Piva R. 2016. Transposable elements: The enemies within. *Experimental Hematology* **44**: 913–916.

Schott S, Coustham V, Simonet T, Bedet C, Palladino F. 2006. Unique and redundant functions of C. elegans HP1 proteins in post-embryonic development. *Dev Biol* **298**: 176–187.

Shi S, Larson K, Guo D, Lim SJ, Dutta P, Yan S-J, Li WX. 2008. Drosophila STAT is required for directly maintaining HP1 localization and heterochromatin stability. *Nat Cell Biol* **10**: 489–496.

Stein GS, Montecino M, van Wijnen AJ, Stein JL, Lian JB. 2000. Nuclear structure-gene expression interrelationships: implications for aberrant gene expression in cancer. *Cancer Res* **60**: 2067–2076.

Thompson PJ, Macfarlan TS, Lorincz MC. 2016. Long Terminal Repeats: From Parasitic Elements to Building Blocks of the Transcriptional Regulatory Repertoire. *Mol Cell* **62**: 766–776.

Vad-Nielsen J, Nielsen AL. 2015. Beyond the histone tale: HP1α deregulation in breast cancer epigenetics. *Cancer Biology & Therapy* **16**: 189–200.

Vakoc CR, Mandat SA, Olenchock BA, Blobel GA. 2005. Histone H3 lysine 9 methylation and HP1gamma are associated with transcription elongation through mammalian chromatin. *Mol Cell* **19**: 381–391.

Velazquez Camacho O, Galan C, Swist-Rosowska K, Ching R, Gamalinda M, Karabiber F, De La Rosa-Velazquez I, Engist B, Koschorz B, Shukeir N, et al. 2017. Major satellite

repeat RNA stabilize heterochromatin retention of Suv39h enzymes by RNA-nucleosome association and RNA:DNA hybrid formation. *Elife* **6**.

Weisend CM, Kundert JA, Suvorova ES, Prigge JR, Schmidt EE. 2009. Cre activity in fetal albCre mouse hepatocytes: Utility for developmental studies. *Genesis* **47**: 789–792.

Wolf G, Yang P, Füchtbauer AC, Füchtbauer E-M, Silva AM, Park C, Wu W, Nielsen AL, Pedersen FS, Macfarlan TS. 2015. The KRAB zinc finger protein ZFP809 is required to initiate epigenetic silencing of endogenous retroviruses. *Genes Dev* **29**: 538–554.

Yang P, Wang Y, Macfarlan TS. 2017. The Role of KRAB-ZFPs in Transposable Element Repression and Mammalian Evolution. *Trends Genet* **33**: 871–881.

Zeeshan H, Lee G, Kim H-R, Chae H-J. 2016. Endoplasmic Reticulum Stress and Associated ROS. *International Journal of Molecular Sciences* **17**: 327.

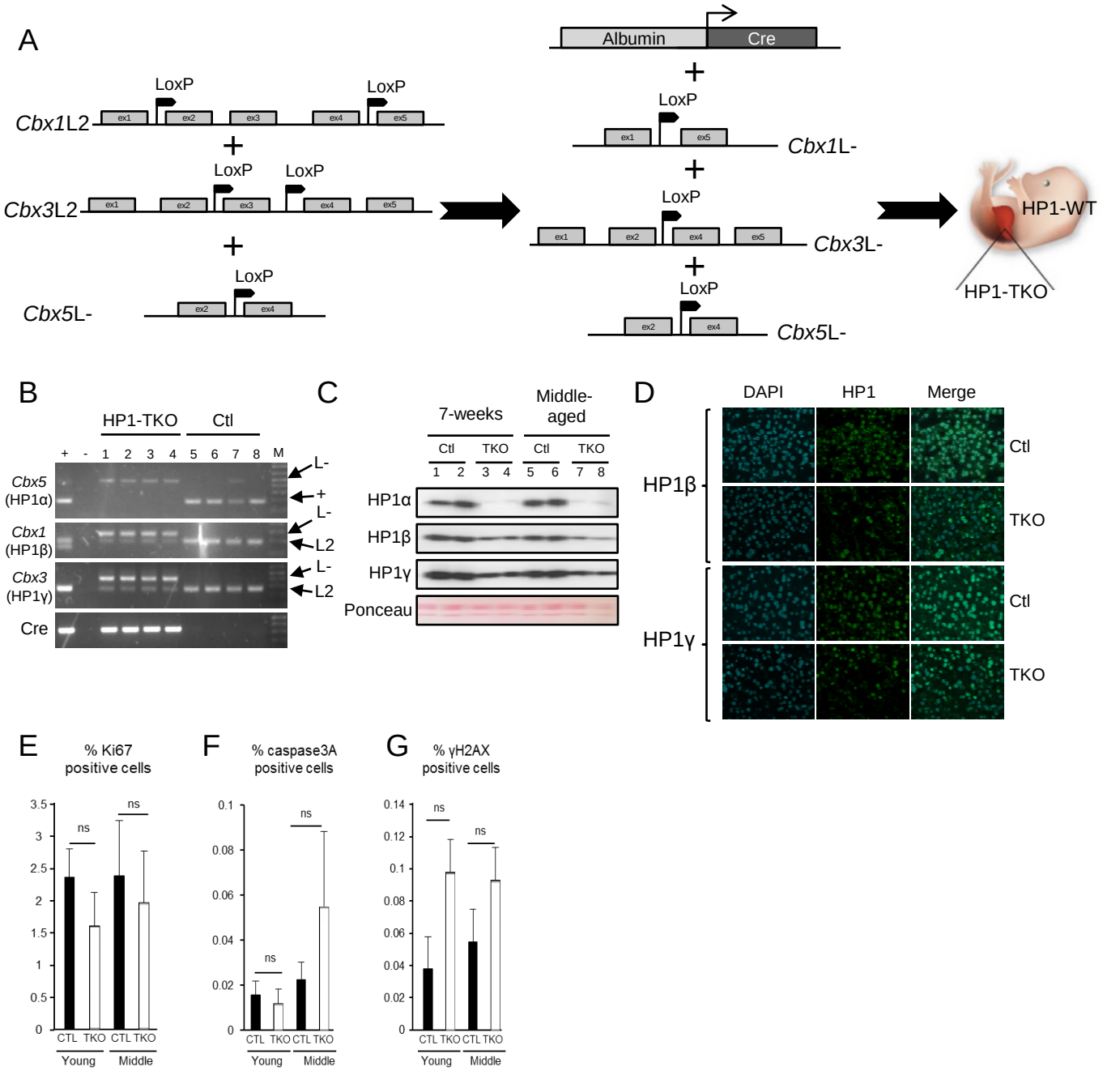

Figure 1: HP1are not required for hepatocyte survival and for liver organization and function. (A) Schematic representation of the strategy to ablate the three HP1-encoding genes (*Cbx1*, *3* and *5*) specifically in hepatocytes using the recombinase Cre expressed under the control of the albumin promoter. For details see *Methods* section. (B) The hepatocyte-specific excision (L- alleles) of the *Cbx1* (HP1β) and *Cbx3* (HP1γ) genes and ubiquitous excision of *Cbx5* (HP1α) only in HP1-TKO (1-4) mice (n=4) compared with control littermates (n=4) (L2 alleles) (5-8) was verified by PCR. Note that control #7 is *Cbx5*$^{L-/+}$. (C) Western blot analysis of whole-cell extracts from liver samples confirmed the absence of HP1α and the decreased expression of HP1β and HP1γ, due to the hepatocytes-specific excision of the corresponding genes, in age-matched HP1-TKO and control mice. Ponceau staining was used as loading control. Young, 7 week-old mice; middle-aged, 3-6-month-old mice. (D) Immunofluorescence analysis of liver tissue cryosections confirmed the absence of HP1β and HP1γ expression in about 60% of cells in young HP1-TKO mice compared with controls. (E-G) Immunohistochemistry analysis of paraffin-embedded liver sections revealed no significant difference in proliferation (Ki67), apoptosis (caspase 3A), and DNA damage (γH2AX) between HP1-TKO (n=5 7-week-old and n= 5 3-6month-old mice) and control mice (n=7 7-week- and n= 4 3-6-month-old mice). Data were normalized to the total number of cells in each section and are shown as the mean ± SEM. ns, no significant difference (Student's t-test).

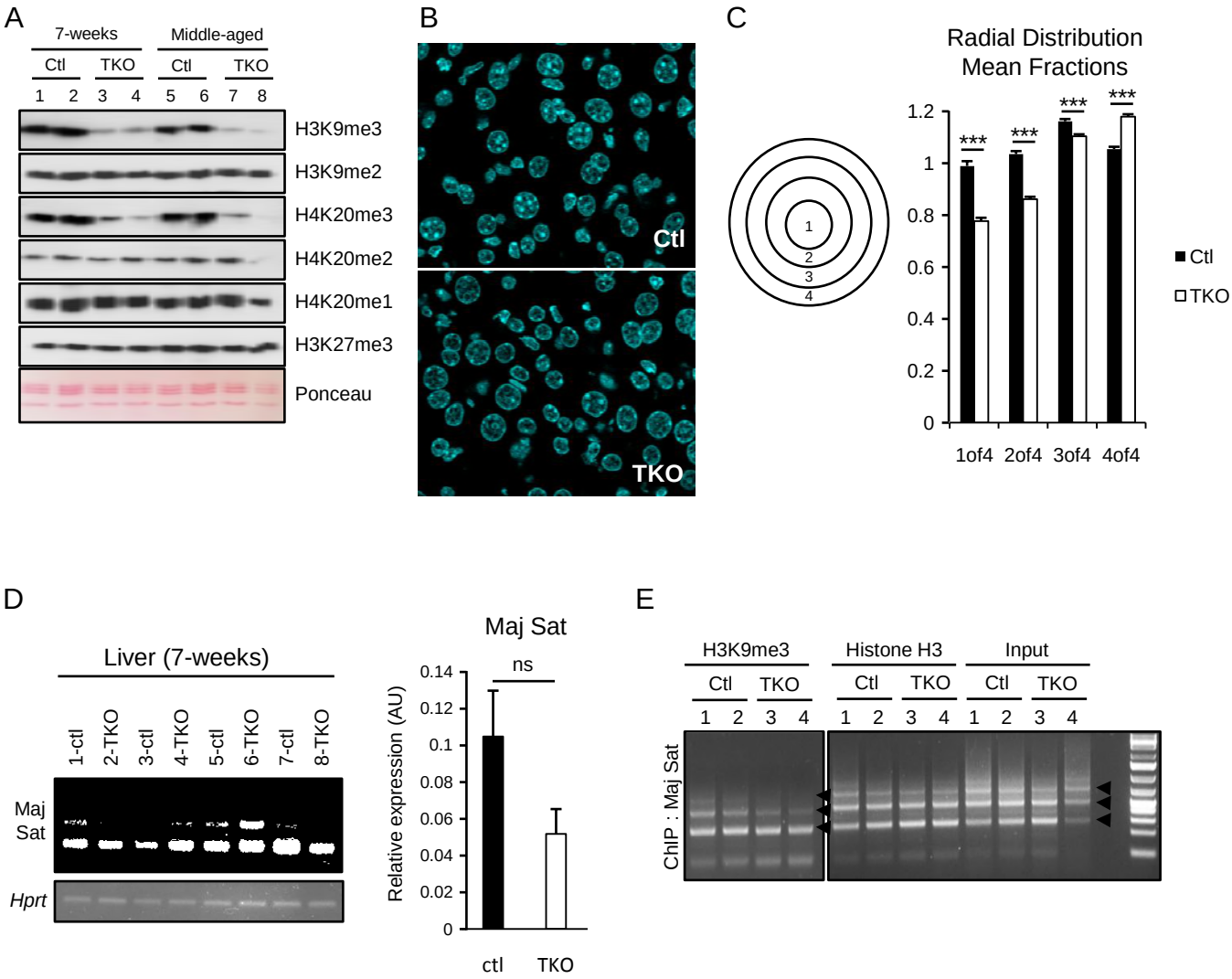

Figure 2: HP1 are essential for heterochromatin organization. (A) HP1 are essential for the maintenance of the two heterochromatin hallmarks H3K9me3 and H4K20me3 in hepatocytes. Western blot analysis of nuclear extracts from liver of 7-week-old and 3-6-month-old controls (Ctl: 1; 2; 5; 6) and HP1-TKO (TKO: 3; 4; 7; 8) mice with antibodies against the indicated histone marks. Ponceau staining was used as loading control. (B) Loss of HP1 leads to a partial relocation of DAPI-dense regions (arrows) towards the nuclear periphery. Representative images of paraffin-embedded liver tissue sections from 7-week-old control (Ctl) and HP1-TKO (TKO) mice stained with DAPI (63x magnification). (C) To select mostly hepatocytes, only the largest nuclei with a size comprised between 70 and 150 μm^2 and with a circular shape were selected for this analysis. 2D sections of nuclei were divided in four concentric areas (1 to 4) and DAPI staining intensity was quantified using the cell profiler software. The mean fractional intensity at a given radius was calculated as the fraction of the total intensity normalized to the fraction of pixels at a given radius in n=584 control and n=762 HP1-TKO (TKO) nuclei. Data are the mean ± SEM. ***p value <0.001. (D) Loss of the three HP1 proteins in hepatocytes does not affect the expression of major satellites. PCR assays (agarose gel on the left) and quantification (histogram on the right) were performed using total RNA from livers of 7-week-old control (1; 3; 5 and 7) and HP1-TKO (2; 4; 6 and 8) mice (n=4/each). (E) H3K9me3 recruitment is reduced on major satellite repeats in the absence of HP1. ChIP assays performed using anti-H3K9me3 and anti-H3 (control) antibodies and liver chromatin from 7-week-old control (Ctl: 1 and 2) and HP1-TKO (3 and 4) animals and analyzed by semi-quantitative PCR.

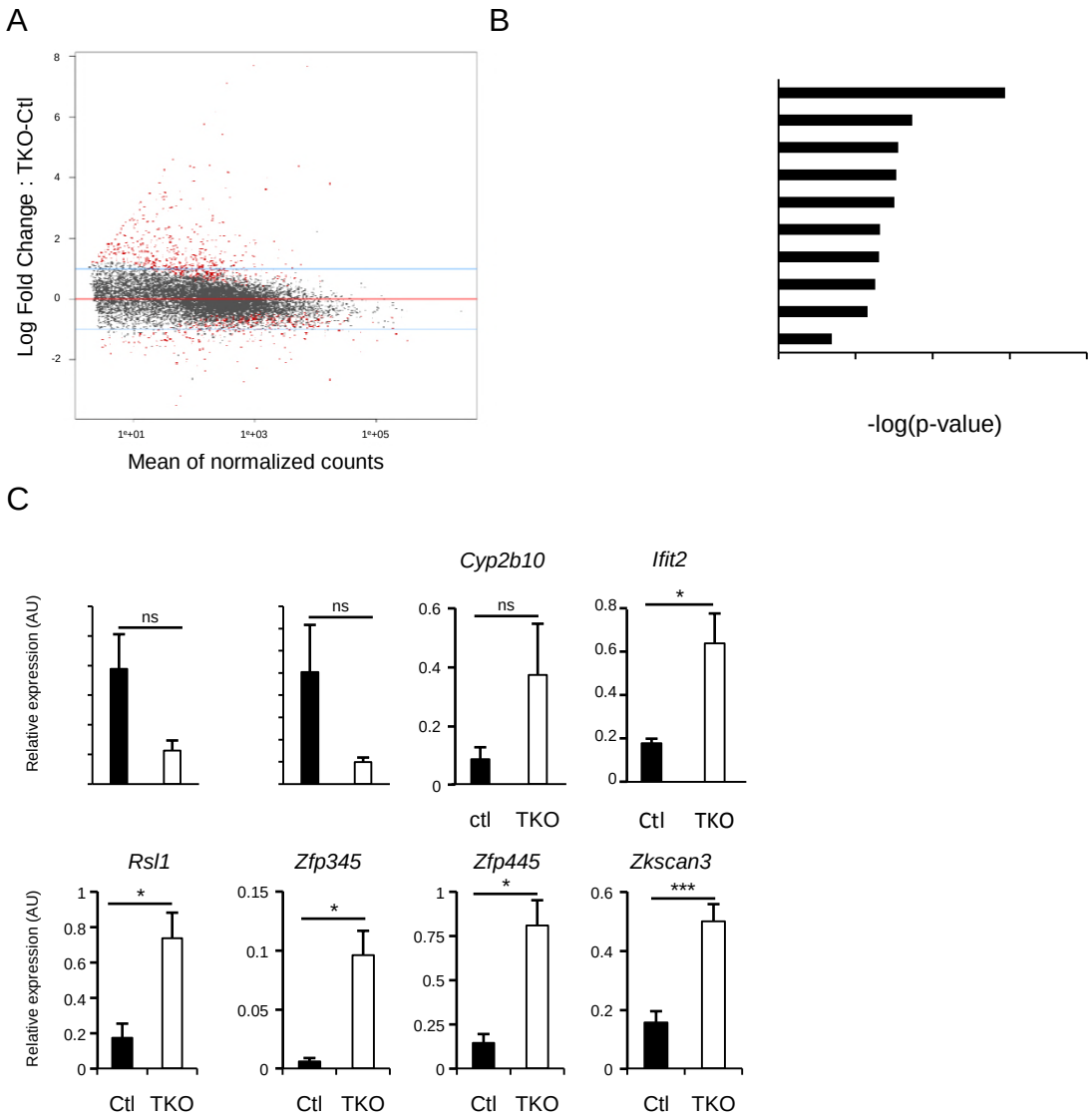

Figure 3: HP1 are essential regulators of gene expression in liver. (A) MA plot after DSeq2 normalization of RNA-seq data for liver RNA samples from of 7-week-old control (n=3) and HP1-TKO mice (n=4). Red dots represent genes that are differentially expressed between controls and HP1-TKO mice (adjusted p-value p <0.05). (B) Functional analysis of the differentially expressed genes using the DAVID Gene Ontology software showed a significant enrichment of KRAB-ZFP-encoding genes and of several families of genes with critical functions in liver homeostasis. (C) Validation by RT-qPCR of the altered expression in 7-week-old HP1-TKO mice of some of the genes identified with the RNA-seq analysis. Data were normalized to *Hprt* expression and are shown as the mean ± SEM. Controls (n=4), HP1-TKO (n=4). ns, no significant difference *p value <0.05; ***p value <0.001 (Student's t-test).

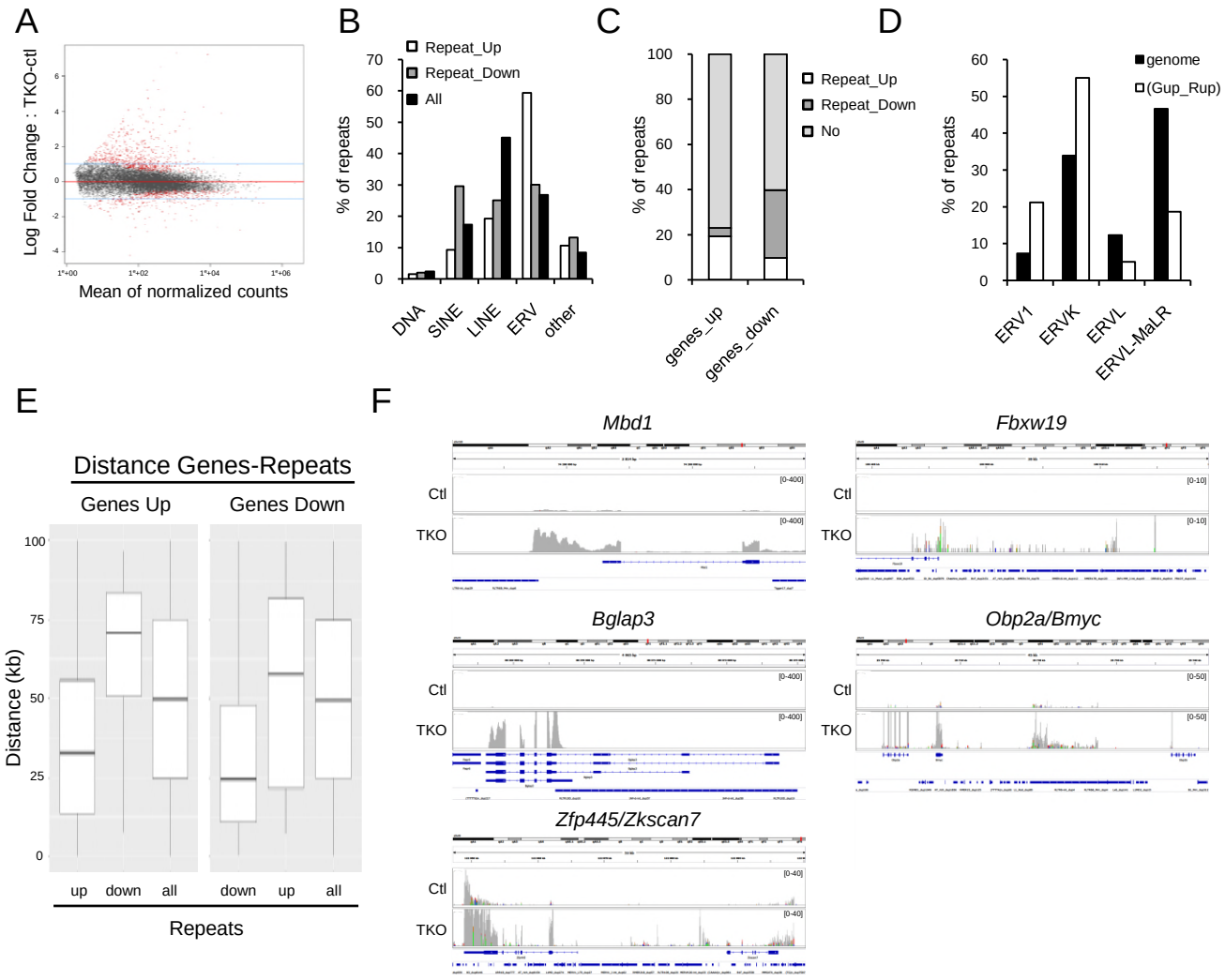

Figure 4: HP1 are required for silencing specific endogenous retroviruses (ERVs) in hepatocytes. (A) MA-plot after DSeq2 normalization of RNA-seq reads aligned against the Repbase database. Red dots represent ERVs that are differentially expressed between controls and HP1-TKO liver samples ($p<0.05$). (B) ERVs are overrepresented in repeats that are upregulated upon loss of HP1α, β and γ (Repeat_Up) compared with repeats that are downregulated (Repeat_Down) and with the genome-wide distribution of repeats according to the RepeatMasker database (All). (C) Repeats overexpressed in HP1-TKO liver samples compared with controls (Repeat_Up) are overrepresented in regions (± 100kb) around genes that are overexpressed in HP1-TKO (genes_up). Conversely, repeats downregulated in HP1-TKO liver samples compared with controls (Repeat_Down) are overrepresented in regions (± 100kb) around genes repressed in HP1-TKO (genes_down). (D) Upregulated ERVs associated with upregulated genes (Gup_Rup) in HP1-TKO livers are enriched in the ERV1 and ERVK sub-families, whereas the ERVL and ERVL-MaLR sub-families are under-represented compared with the genome-wide distribution of these repeats. (E) Repeats that are upregulated or downregulated upon HP1 protein loss tend to be closer to genes that are up- or down-regulated in HP1-TKO, respectively. The absolute distance (in base pairs) was measured from the gene transcriptional start site and from the beginning of the repeat, according to the RepeatMasker annotation. (F) Representative Integrative Genomic Viewer snapshots of the indicated upregulated genes associated with upregulated repeat sequences.

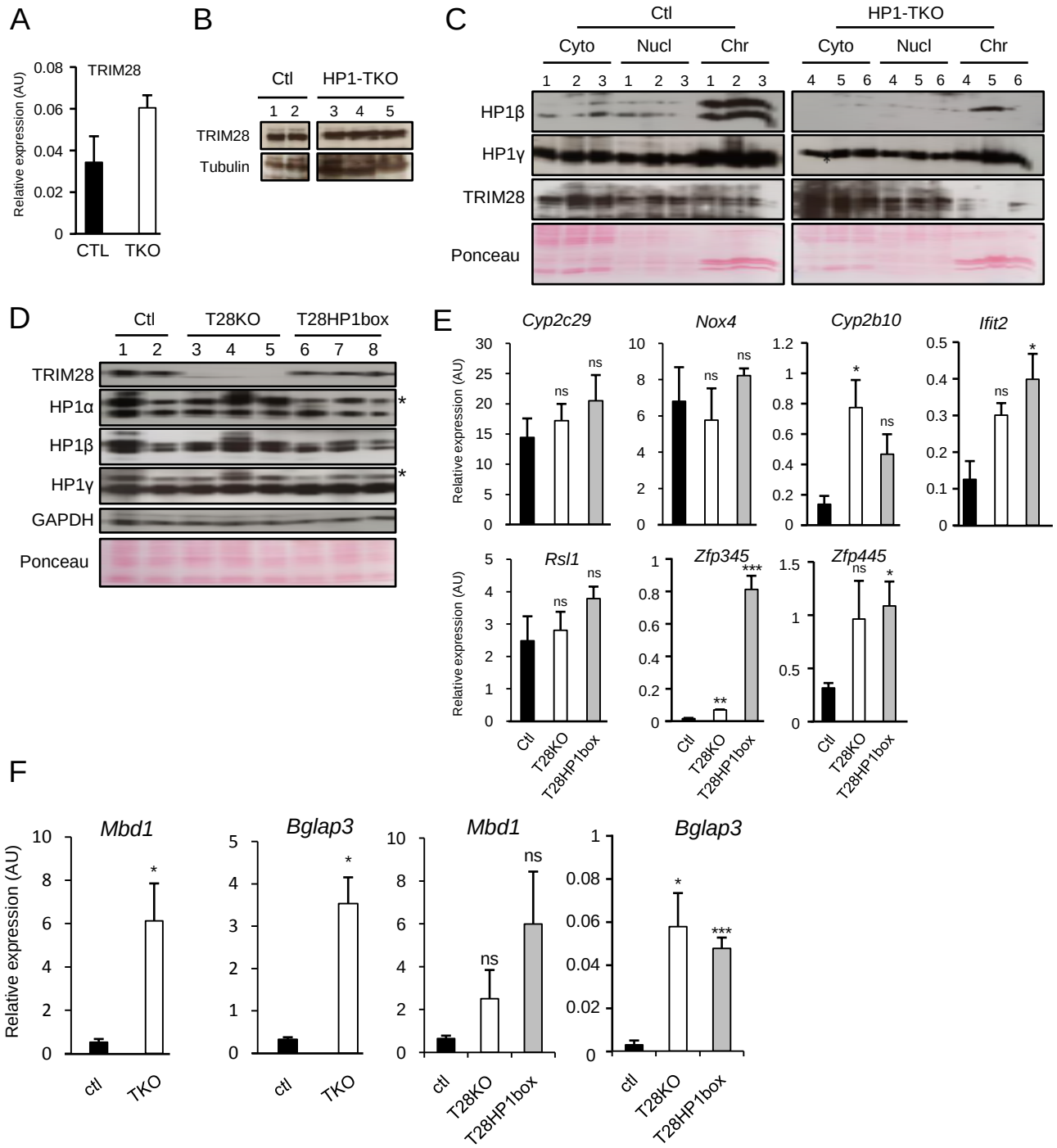

Figure 5: HP1 proteins are involved in the recruitment and/or maintenance of TRIM28 at chromatin in hepatocytes. (A) TRIM28 expression is independent of HP1 proteins. RT-qPCR quantification of TRIM28 expression in total RNA from livers of 7-week-old control (n=4) and HP1-TKO (TKO; n=4) mice. Data were normalized to *Hprt* expression and are shown as the mean ± SEM. (B) Western blot analysis of 50µg of whole cell extracts from livers of x-week-old control (1 and 2) and HP1-TKO (3 to 4) mice using an anti-TRIM28 polyclonal antibody. Tubulin was used as loading control. (C) HP1 are required for the stable association of TRIM28 to chromatin. Cytosolic (Cyto), nuclear (Nucl) and chromatin (Chr) extracts from livers of x-week-old control (1 to 3) and HP1-TKO mice (4 to 6) were analyzed by western blotting using the anti-TRIM28 polyclonal antibody. (D) The loss of interaction between TRIM28 and HP1 proteins does not alter the level of expression of TRIM28 and of the HP1 proteins. 50 µg of whole liver extracts from x-week-old controls (n=2), T28KO (n=3) and T28HP1box (n=3) mice were analyzed by western blotting using the anti-TRIM28 polyclonal antibody and anti-HP1α, β and γ monoclonal antibodies. GAPDH and Ponceau staining were used as loading controls. (D) TRIM28 is involved in the regulation of the expression of some but not all HP1-dependent genes. RT-qPCR analysis using liver RNA samples from 5 week-old control (n=5), T28KO (n=5) and T28HP1box (n=5) mice. Data were normalized to *Hprt* expression and are shown as the mean ± SEM. (F) TRIM28 is involved in the regulated expression of HP1- and ERV-dependent genes. Expression of *Mbd1* and *Bglap3* by RT-qPCR analysis using liver RNA samples from 7-week-old control (ctl) and HP1-TKO (TKO) mice, and 5-week-old control (n=5), T28KO (n=5) and T28HP1box (n=5) mice. Data were normalized to *Hprt* expression and are shown as the mean ± SEM. ns, no significant difference *p value <0.05; ***p value <0.001 (Student's t-test).

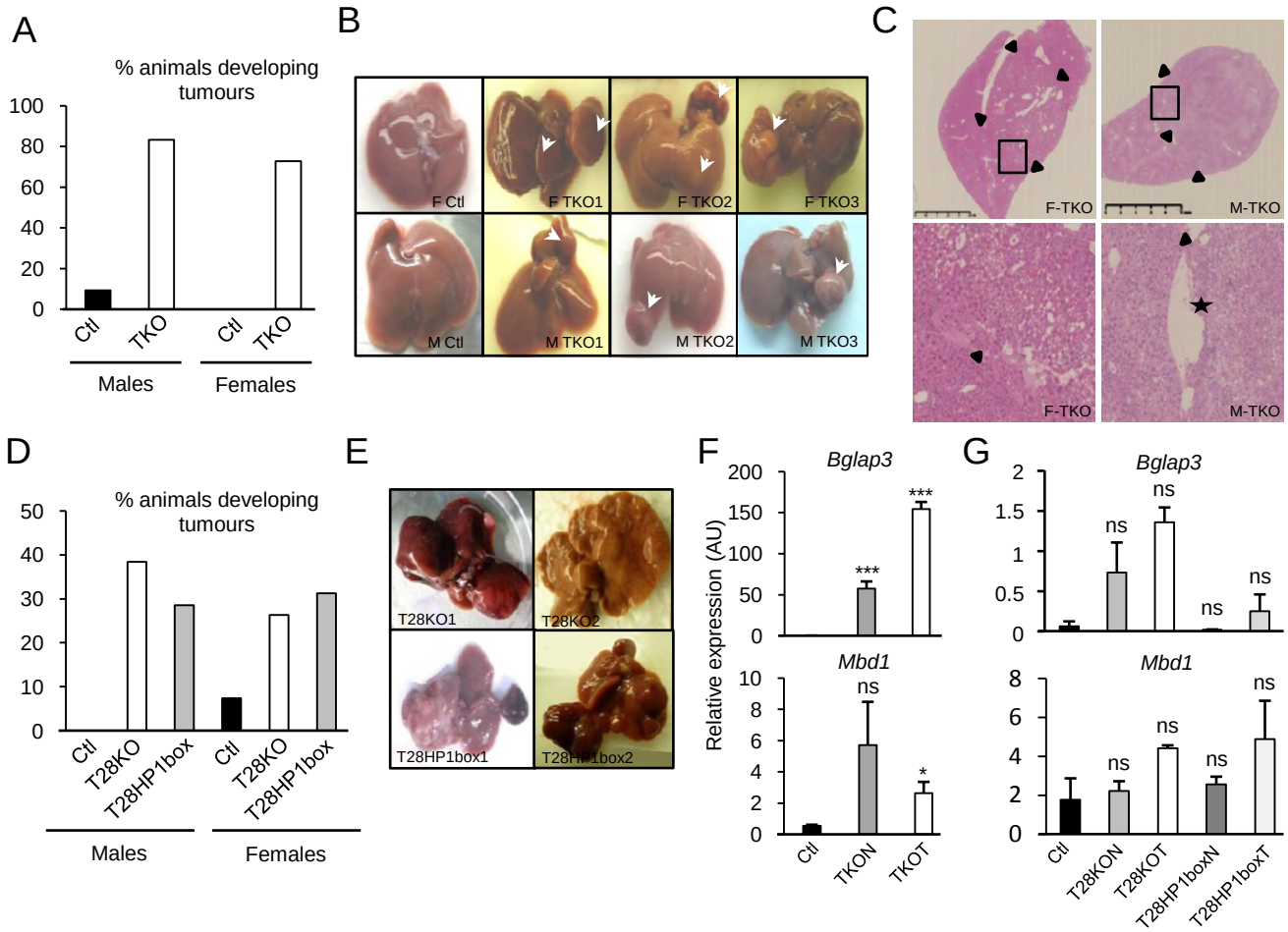

Figure 6: HP1 and their association with TRIM28 prevent tumor development in liver. (A) Controls (n=67) and HP1-TKO (TKO, n=17) animals older than one year of age were sacrificed and the percentage of animals with tumors (morphological and histological analysis) was calculated. (B) Morphology of the livers with tumors (arrows) in three HP1-TKO females (F TKO1, 2 and 3) and three HP1-TKO males (M TKO1, 2 and 3) older than one year of age. The liver morphology of one age-matched control female and male is also shown (F Ctl and M Ctl, respectively). (C) Liver histological analysis (hematoxylin-eosin-Safran staining) of one representative HP1-TKO female (F-TKO) and one representative HP1-TKO male (M-TKO). Upper panels: tumor/liver parenchyma interface highlighted by arrowheads (low magnifications). Bottom panels: magnification (x 100) of the boxes in the upper panels showing the tumor in the right part of the images (thick plates of atypical hepatocytes). A venous tumor thrombus is also present (asterisk). (D) The association between TRIM28 and HP1 is essential in hepatocytes to prevent liver tumor development. Control (n=42), T28KO (n=32) and T28HP1box (n=30) mice older than one year of age were sacrificed and the percentage of animals with tumors (morphological and histological analysis) was calculated. (E) Liver histological analysis (hematoxylin-eosin-Safran staining) of representative animals. (F) The expression of *Bglap3* and *Mbd1* was higher also in livers from old (>1year old) HP1-TKO mice. RT-qPCR analysis was performed using RNA from old control (n=7), and HP1-TKO liver samples (TKON for normal part, TKOT for tumor part) (n=7). (G) The alteration of *Mbd1* and *Bglap3* expression upon loss of the association between TRIM28 and HP1 proteins was not maintained in old animals. RT-qPCR analysis using RNA from control (n=5), T28KO (T28KON for normal part, T28KOT for tumor part) (n=5) and T28HP1box (T28HP1boxN for normal part, T28HP1boxT for tumor part) livers (n=5). Data were normalized to *Hprt* expression and are shown as the mean ± SEM. ns, no significant difference *p value <0.05; **p value <0.01; ***p value <0.001 (Student's t-test).

Table 1: HP1-dependent p450 genes.

Gene name	Log2 fold-change	padj	Redox	Endoplasmic reticulum	Drug metabolism	Lipid metabolism	Steroid synthesis
Cyp2b10	4.06	1.41E-38	1	1	0	0	1
Cyp2b9	2.68	4.51E-10	1	1	0	0	1
Cyp2b13	1.80	0.000120	0	0	0	0	1
Cyp4f16	1.63	1.36E-09	0	0	0	0	0
Cyp2d12	1.38	0.000468	0	0	0	0	1
Cyp2a4	1.09	0.0342	0	0	0	0	0
Cyp2a22	1.06	0.000559	0	0	0	0	0
Cyp2f2	-0.65	0.00318	1	1	0	0	0
Cyp4f13	-0.67	0.0151	0	0	0	0	0
Cyp2r1	-0.72	0.0173	1	1	0	0	0
Cyp27a1	-0.83	1.30E-05	1	0	0	0	0
Cyp2d37-ps	-0.83	0.0319	0	0	0	0	0
Cyp3a25	-0.85	0.00222	1	1	0	0	1
Cyp39a1	-0.88	0.00164	1	1	0	1	0
Cyp2e1	-0.94	7.81E-05	1	1	1	0	1
Cyp2d26	-0.95	2.57E-05	1	1	0	0	1
Cyp2a5	-0.97	0.00129	0	0	0	0	0
Cyp2d13	-1.00	0.00445	0	0	0	0	0
Cyp1a2	-1.25	3.65E-12	1	1	1	1	1
Cyp2c53-ps	-1.31	0.01178	0	0	0	0	0
Cyp2d40	-1.42	6.83E-06	0	0	0	0	1
Cyp46a1	-1.64	0.000629	1	1	0	1	0
Cyp3a59	-2.15	3.62E-17	1	0	0	0	0
Cyp2c44	-2.20	2.18E-20	0	0	0	0	1
Cyp2c29	-2.60	7.65E-25	1	1	0	0	1

(1) found and (0) not found according to the David Gene Ontology software.